Title	Oriented growth of metal and semiconductor nanostructures within aligned mesoporous channels
Authors	Petkov, Nikolay;Platschek, Barbara;Morris, Michael A.;Holmes, Justin D.;Bein, Thomas
Publication date	2007-02-21
Original Citation	Petkov, N., Platschek, B., Morris, M. A., Holmes, J. D. and Bein, T. (2007) 'Oriented Growth of Metal and Semiconductor Nanostructures within Aligned Mesoporous Channels', Chemistry of Materials, 19(6), pp. 1376-1381. doi: 10.1021/cm0627239
Type of publication	Article (peer-reviewed)
Link to publisher's version	https://pubs.acs.org/doi/abs/10.1021/cm0627239 - 10.1021/cm0627239
Rights	© 2007 American Chemical Society. This document is the Accepted Manuscript version of a Published Work that appeared in final form in Chemistry of Materials, copyright © American Chemical Society after peer review and technical editing by the publisher. To access the final edited and published work see https://pubs.acs.org/doi/abs/10.1021/cm0627239
Download date	2024-05-13 00:16:15
Item downloaded from	https://hdl.handle.net/10468/8142

Oriented Growth of Metal and Semiconductor Nanostructures within Aligned Mesoporous Channels

Nikolay Petkov[1], Barbara Platschek[2], Michael A. Morris[1], Justin D. Holmes[1]* and Thomas Bein[2]*

[1]Department of Chemistry, Materials Section and Supercritical Fluid Centre, University College Cork, Cork, Ireland

[2]Department of Chemistry and Biochemistry, University of Munich, Butenandtstr. 11, 81377 Munich, Germany.

To whom correspondence should be addressed: e-mails: j.holmes@ucc.ie; bein@lmu.de

RECEIVED DATE (to be automatically inserted after your manuscript is accepted if required according to the journal that you are submitting your paper to)

ABSTRACT In the present work we show how different types of inclusion chemistry can be used to generate oriented, high aspect-ratio metal and semiconductor nanowires in insulating silica host structures prepared within anodic alumina membranes (AAMs). The structural features of the Pluronic123-templated silica filaments in the AAMs with their intriguing columnar and circular arrangement of mesopores allow for the inclusion of a variety of aligned 1D nanostructures ranging from metallic (Pt, Au and Pd), semiconductor (Ge) to carbon nanotubes and filaments. The synthetic techniques include wet chemical impregnation and reduction in pre-calcined mesopores, impregnation of surfactant-containing mesopore systems, and mass transport *via* supercritical fluid deposition in surfactant-containing mesopores. Important issues such as the crystallinity and continuity of the encapsulated wires as a function of material and deposition technique have been discussed.

KEYWORDS Alignment, mesoporous silica channels, nanowires, anodic alumina, metals and semiconductors.

BRIEFS In the present work we show how different types of inclusion chemistry can be used to generate oriented, high aspect-ratio metal and semiconductor nanowires in insulating silica host structures deposited within anodic alumina.

MANUSCRIPT TEXT

Introduction

Alternative non-lithographic methodologies for constructing the smallest mesoscopic features in integrated circuits will soon be needed.[1] One promising non-lithographic strategy is the use of solution phase chemistry to promote the self-assembly of materials from precursor 'building blocks' into complex hierarchical mesoscopic architectures.[2] Mesoporous materials with well-defined periodic channel systems, having channel diameters below 10 nm, can host and guide the growth of a variety of 1D nanostructures.[3] However, because of difficulties in reproducibly preparing easily accessible and oriented mesostructured domains, they have found limited use as templates for nanowires. For example, during the preparation of mesostructured thin films (MTFs), highly oriented structures on a substrate have been obtained but the most frequently achieved phases show hexagonally ordered channels aligned with the long axis parallel to the substrate surface.[4] Other mesophase structures such as 3D cubic or hexagonal assembled from spherical micelles have also been prepared in the form of thin films and were utilized as hosts for forming ordered arrays of metal nanoparticles.[5,6]

Anodic alumina membranes (AAMs) can serve as alternative templates for nanostructured materials; they have been widely used as hosts for forming ordered arrays of vertically aligned carbon nanotubes, metal and semiconductor nanowires.[7-11] However, AAMs tend to have large pore diameters above 10 nm and often inferior pore ordering and pore-size distributions in comparison to the mesoporous materials.

Recently, we and others have shown that the highly anisotropic pore structure of the AAMs can be combined with methods for preparing silica MTFs to obtain highly aligned mesostructured domains inside the channels of the AAMs.[12-14] In this paper we show that these hierarchical structures can be used as hard templates to host and guide the growth of aligned and ordered metal and semiconductor 1D nanostructures. Noble metals such as Pt, Pd and Au were deposited inside the mesopores either by direct wet impregnation followed by reduction, or alternatively by chemical modification of the mesoporous surface, followed by metal salt complexation and reduction. Semiconductor Ge nanostructures were deposited by solvent assisted supercritical fluid (SCF) technique pioneered in one of our groups for the growth of semiconductor nanostructures in AAMs.[15] A similar supercritical fluid technique has already been used for the deposition of carbon nanostructures in analogous mesostructured templates.[16]

Experimental Section

Synthesis

The deposition mixtures for mesoporous silica were prepared by applying a two-step synthesis procedure. First, 2.08 g tetraethyl orthosilicate (TEOS, Aldrich) was mixed with 3 g of 0.2 M HCl, 1.8 g H_2O and 5 mL EtOH and heated at 60 °C for 1 h to accomplish acid-catalyzed hydrolysis-condensation of the silica precursor.

For the preparation of the Pluronic123-containing solutions, the pre-hydrolyzed silica was mixed with 15 ml 5 wt% ethanol solutions of poly(ethylene oxide)-b-poly(propylene oxide)-b-poly(ethylene oxide) tri-block copolymer, Pluronic123. To this mixture, NH_4Cl with a TEOS: NH_4Cl molar ratio of 0.30 was added by dissolving the inorganic salt in the ethanol solutions. The resulting deposition mixtures were aged for 2 h at room temperature and used for the deposition of the silica/surfactant nanostructures in the AAMs. The AAMs (47 mm, Anodisc[TM], Whatman) with nominal pore diameters of 200 nm and a thickness of approximately 60 µm were soaked with the prepared precursor mixture by dropping 0.75 mL over the whole membrane surface. After 2 hours at room temperature the membrane appeared dry

and homogeneously soaked with the synthetic mixture. The composite membranes were calcined in flowing air at 550 °C for 4 h (ramping 0.75 deg/min).

In order to introduce Pt-nanostructures in the composite membranes, calcined samples were repeatedly impregnated with aqueous 0.1 wt% $Pt(NH_3)Cl_2$ solutions at 100 °C. Highest loadings with Pt were achieved after at least 5 times impregnation-drying cycles. Finally, the Pt-loaded samples were reduced in flowing 5 v/v% H_2/N_2 mixture at 300°C for 2 h, resulting in a black color of the samples.

Au-encapsulation was done on calcined, aminopropyltriethoxysilane (APES - Fluka) modified silica/AAM that was impregnated with 30 mM $H[AuCl_4].3H_2O$ at room temperature for 24 h. After washing in de-ionized water the samples were left in air at room temperature for a week. Under these conditions and due to the presence of amine functionalities, gold reduction takes place, resulting in a profound change in the color of the samples from light yellow to red-orange, dark red and finally violet.

Pd-loading was done on non-calcined membranes by repeated impregnation with 0.75 mM $Pd(NH_3)(NO3)_2$ water/ethanol solution at 60 °C. The conditions of the Pd-impregnation resulted in a direct reduction of the Pd precursor and a black color of the samples.

Ge-nanostructures were grown by degradation of diphenyl germane in supercritical hexane at 380 °C and 70 bar for 30 min. Non-calcined composite membranes were placed in a 25 mL high pressure cell under an ambient atmosphere, and the cell was connected to a pressure meter through a three-way valve. After the reaction the cell was cooled down to room temperature and the samples (black in color) were removed and washed with acetone.

In some cases the composite membranes were first thinned by double-side polishing (as described in the characterization section) and then were subjected to only one impregnation cycle. In this case better loading is achieved even after one impregnation cycle.

Characterization

The TEM images were obtained with a JEOL 2010 transmission electron microscope operating at 200 kV. The elemental compositions were determined with a JEOL 5510 instrument equipped with an

Oxford EDX detector. Samples for electron microscopy were prepared by the following methods: (i) the alumina matrix was dissolved in phosphoric acid to release the embedded mesoporous silica; (ii) plan-views and cross-sections were prepared by dimple grinding, followed by Ar-ion polishing. The precision Ar-ion polishing was done at grazing angles of 6° with 5 kV acceleration voltage with a Gatan Precision ion polishing system, Model 691. The surface morphology of the samples was determined with scanning electron microscopy (SEM) with a JEOL JSM 6500 microscope.

Results and Discussion

The present method for the self-assembly of the ordered silica/surfactant nanocomposites in the channels of AMMs is described in detail in a previous report.[14] Briefly, commercial AAMs with nominal pore sizes of approximately 200 nm were soaked with precursor mixtures containing Pluronic123 as a structure directing agent, hydrolyzed silica and salt (for details see Experimental). Upon solvent evaporation, the concentration of surfactant micelles in the solution increases and subsequent condensation of silica around these micelles results in the formation of the ordered mesoporous phases in the channels of the AAMs. Typically two types of mesopore orientation in the AAM-channels can be identified. One, usually referred to as "circular", can be envisioned as composed of concentric mesophase channels, hexagonally ordered in the direction of the long axis of the filaments. The direct observation of this mesophase structure is illustrated by plan-view and cross-sectional TEM images shown in Figure 1(a) and (b). Note that this kind of mesophase structure is rather unusual for 3D crystals because of the lack of extended 3D order, giving them the name "circulites" or circular crystals.[17] The other observed mesophase structure is composed of hexagonally ordered columnar mesopores aligned parallel to the long axis of the filaments. Figure 1(c) and (d) depicts typical examples of such structures imaged perpendicularly and parallel to the membrane surface. Usually these two distinct mesophase structures can be observed in neighboring channels of the AAMs with different ratios of "circular" to "columnar" orientations. However, enhanced control of the mesophase structures can be achieved by changing the ionic strength of the deposition mixtures (introduction of inorganic

5

salts, see Experimental for relevant experimental procedures), the relative humidity during the deposition, and the silica-to-surfactant ratio. A detailed description of these observations is presented in a separate report.[18]

The embedded silica/surfactant nancomposite mesophases obtained here differ significantly from those reported previously for confined polymer systems.[19] The silica-based mesostructures form a rigid silica framework upon removal of the surfactant, leaving solid supports with ordered porosity that can offer a template-matrix for guided growth of different conductive structures. Recent research on the 1D confinement of conductive nanostructures has shown that control over alignment and structural complexity is essential for the incorporation of these structures into integrated electrical circuits.[20,21] Here we show that aligned noble metal and semiconductor nanostructures can be prepared in the oriented silica mesopores embedded within the channels of the AAMs.

For example, Pt-nanostructures were deposited by a wet chemical impregnation technique followed by hydrogen-reduction at 300 °C (for details see Experimental). Figure 2(a) shows a representative plan-view image of the calcined mesoporous support, having vertically aligned columnar mesopores with incorporated Pt-nanostructures. Despite the shrinkage of the mesoporous support in a direction perpendicular to the alumina walls (Figure 2a), the hexagonal order is still retained resulting in an ordered arrangement of Pt-nanostructures. When the silica/Pt nanostructures are imaged in the direction perpendicular to the mesoporous channels, after the dissolution of the alumina matrix, well-defined Pt-nanowires running along the long axis of the mesoporous silica nano-filaments are observed (inset in Figure 2a). The mean diameter of the nanowires is approximately 5.5 nm. They feature well-defined crystalline fringes of Pt with a d-spacing of the (111) planes of about 0.24 nm, calculated from fast Fourier transforms (FFTs) of the corresponding HRTEM images (Figure 2b). The uniform diameter and the arrangement of the Pt-nanostructures (separated and isolated by the silica walls) confirm that their growth is guided by the arrangement of the meso-channels. The dimensions of the encapsulated Pt-nanostructures extend to several hundreds of nanometers and they appear to be composed of small

6

segments (10-20 nm) thus forming chain-like nanowires. This type of morphology is commonly observed for metal nanostructures prepared in mesoporous materials by repeated wet impregnation.[22]

A similar synthetic approach was used for the deposition of Au-nanostructures, with the notable difference that the surface of the meso-channels was modified, prior to Au-deposition, with organo-silane molecules containing primary amino groups (for details see Experimental). In a second step the template was wet-impregnated with aqueous $H[AuCl_4]$ and, after washing in deionized water, was left in air at room temperature for a week. Under these conditions and due to the presence of amine functionalities, gold reduction takes place, resulting in a profound change in the color of the samples from light yellow to red-orange, dark red and finally violet. These changes can be explained by the increase of the particle size of the gold nanocrystals with time.[23,24] The choice of these gentle reduction conditions was guided by the fact that high-temperature reduction resulted in the formation of bigger gold crystals on the outer surface of the mesostructured filaments. Figure 2c shows an example of a "circular" mesostructured filament with deposited Au-nanostructures after dissolution of the AAM matrix. In this case, the nanostructures are aligned perpendicular to the long axis of the mesostructured filaments and, when imaged in plan-view, it can be seen that they follow the curvature of the circular silica mesopores (inset in Figure 2c). Thus full or semi-continuous concentric circles of metallic nanostructures isolated by silica walls and hexagonally ordered in a single filament can be prepared. The Au-nanostructures appear to be highly crystalline as seen from the selected area electron diffraction (SAED) and HRTEM image (Figure 2d). Similarly to the Pt inclusion, the Au-nanostructures are composed of small elongated segments which form chain-like curved nanostructures. We note here that we have previously used electroless reduction for the deposition of larger single crystalline domains of Au-nanowires in SBA-15 material[25] – this technique might also be amenable for the preparation of larger crystalline Au-nanostructures in the hierarchical template structures discussed in this article.

The preparation of the above Pt and Au nanostructures relies on the calcination of the mesoporous material prior to inclusion of the metal precursor. Calcination of the mesoporous silica in the AAM channels leads to the contraction of the filaments in directions perpendicular to the walls of the AAMs

7

(Figure 2a). In an alternative approach, Pd-nanostructures were assembled by direct repeated impregnation of the non-calcined samples with water/ethanol solutions of $Pd(NH_3)_4(NO_3)_2$ at 60°C (for details see Experimental). The resulting silica/Pd nanostructures embedded in the alumina matrix and imaged as plan-views are shown in Figure 3(a) and (b). Well-ordered hexagonal arrangements of the Pd-nanostructures encapsulated in the silica framework are observed. The conditions of the Pd-impregnation result in the direct reduction of the Pd precursor complexes to metallic Pd, thus eliminating the necessity of further high temperature reduction. Well-resolved Pd crystalline fringes are observed (Figure 3b) with a d-spacing of about 0.23 nm, determined from FFTs of the HRTEM image (inset in Figure 3b). Apparently at these mild reduction conditions, and without removing the template, a relatively high loading of the mesoporous support is possible (Pd/Si atom ratio of 0.85 in comparison to Pt/Si and Au/Si atom ratios of 0.17 and 0.09, respectively, Figure 3d). When imaged in a direction perpendicular to the long axis of the filaments, well aligned Pd-nanostructures are displayed with diameters of approximately 8 nm. These nanostructures are composed of small separate segments forming chain-like nanowires (inset in Figure 3b). Thus, the non-calcined mesoporous supports with their well-aligned channels facilitate the organization of Pd-nanostructures in the form of highly aligned metallic nanowires. The extension of the latter approach to the encapsulation of other metallic nanostructures inside the porous structure of the silica/surfactant nano-composites within AAMs is currently under investigation.

The three metallic nanostructures discussed so far are characterized by nucleation and growth in various solvents included in the mesopores, including the fluid phase of encapsulated surfactants in the case of Pd. This implies a pattern of mass transfer resulting in limited fill-factors and limited continuity of the deposited materials. In an effort to facilitate mass transfer and enhance the continuity of the encapsulated nanowires, solvent assisted supercritical fluid (SCF) deposition was employed. This technique has been pioneered by one of our groups for the growth of continuous semiconductor nanostructures in mesoporous materials.[15]

The implementation of SCF conditions allows for fast and effective mass transport at almost zero surface tension which is essential for continuous and high loading of the mesopores (see Supporting Information). Figure 3c shows a plan-view TEM image of a non-calcined "columnar" mesostructured filament with encapsulated Ge-nanostructures prepared by supercritical hexane/diphenyl germane inclusion (for details see Experimental). During the deposition the mesostructure organization is preserved, thus leading to an ordered arrangement of semiconductor nanostructures encapsulated in an insolating silica matrix. The diameters of the Ge-nanostructures are limited by the dimensions of the mesoporous channels and are observed to be about 8 nm, in agreement with the pore dimensions of the non-calcined support. In some cases, mesoporous channels with Ge deposited only on the mesoporous walls were observed (shown with arrows on the image) to form nanotube-like structures. This observation is in agreement with the proposed mechanism for nanowire growth in the mesoporous channels by SCF techniques.[26]

The structural features of the Pluronic123-templated silica filaments in the AAMs with their intriguing columnar and circular arrangement of mesopores allow for the inclusion of a variety of aligned 1D nanostructures ranging from metallic (Pt, Au and Pd), semiconductor (Ge) to carbon nanotubes and filaments (as reported previously[16]). There are two noticeable advantages with these structures. First, they are hierarchically aligned due to the quasi-hexagonal order of the channels of the AAMs as well as the ordered structures of the included mesoporous silica filaments. Second, they offer the potential to encapsulate a very high density of conducting nanostructures. For example, a number density of about 6.3×10^8 filaments per cm^2 can be achieved by saturation loading of the channels of the AAMs with mesostructured filaments, giving 1.4×10^{11} nanowires per cm^2. Before these numbers can be achieved, further optimization of the synthetic procedures for both the deposition of the mesostructured filaments and 1D metallic and semiconductor nanostructures is required.

Conclusions

In the present work we show how different types of inclusion chemistry can be used to generate oriented, high aspect-ratio metal and semiconductor nanowires in insulating silica host structures prepared within AAMs. The synthetic techniques include wet chemical impregnation and reduction in pre-calcined mesopores, impregnation of surfactant-containing mesopore systems, and mass transport via supercritical fluid deposition in surfactant-containing mesopores. Important issues such as the crystallinity and continuity of the encapsulated wires as a function of material and deposition technique have been discussed. The proposed hierarchically ordered alumina/silica/material-of-choice nano-composites can be suitable model systems for the electrical characterization of single, insolated 1D nanostructures by conductive AFM-tips. First attempts in this direction were already made in our laboratory on 1D nanostructures prepared in columnar channels of the AAMs.[27] A further reduction of the diameter of these structures by encapsulation in mesoporous templates may lead to future nano-devices beyond the 10 nm node.
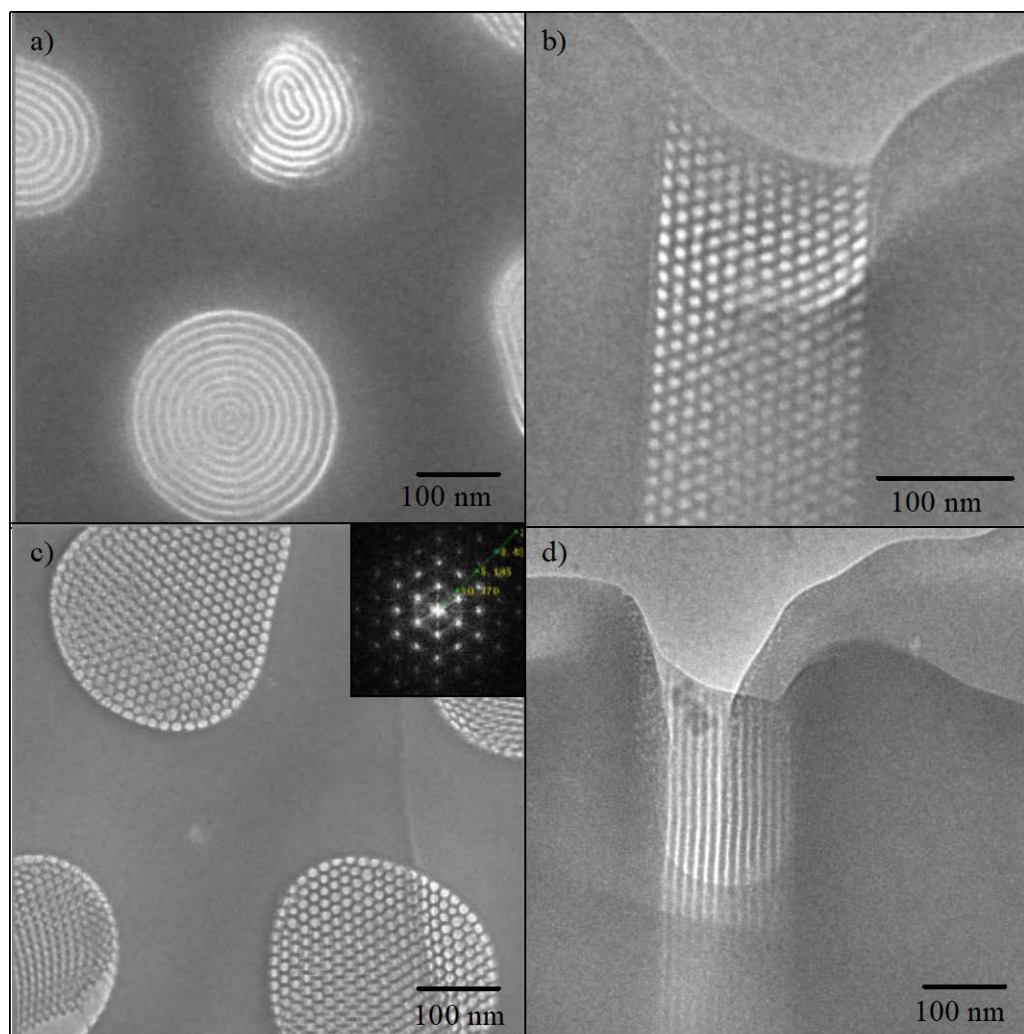
Figure 1. Mesophase morphologies observed in the AAM channels. Top: "Circular" mesophase structures, hexagonally ordered in the direction of the long axis of the filaments, showing a) plan- and b) side-view TEM images. Bottom: "columnar" mesophase structures, hexagonally ordered in the plane of the substrate, showing c) plan- and d) side-view TEM images (inset: FFT for one of the filaments shown in Figure 1c).
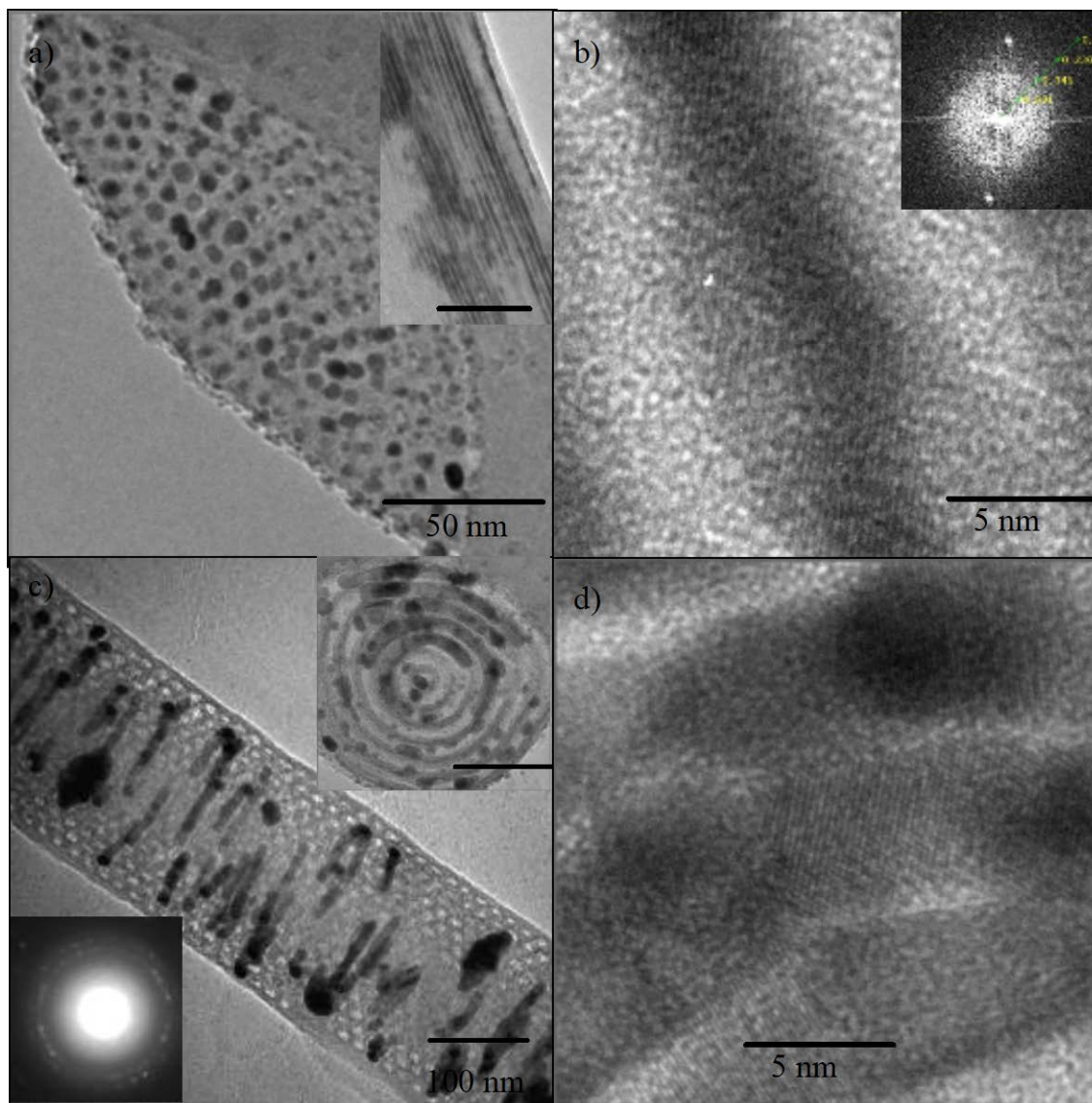
Figure 2. Platinum and gold nanostructures prepared in calcined mesostructured filaments. a) Plan-view TEM image of Pt-nanostructures (inset: side-view TEM image after dissolving the alumina matrix, scale bar 100 nm) and b) HRTEM image of the Pt-nanostructures in an isolated mesostructured filament (inset: corresponding FFT), c) Side-view TEM image of Au-nanostructures prepared in calcined, silane –modified "circular" mesostructured filaments, after dissolving the alumina matrix (insets: corresponding SAED and plan-view TEM image, scale bar 50 nm), and d) plan-view HRTEM image of the Au-nanostructures in "circular" mesostructured filaments.
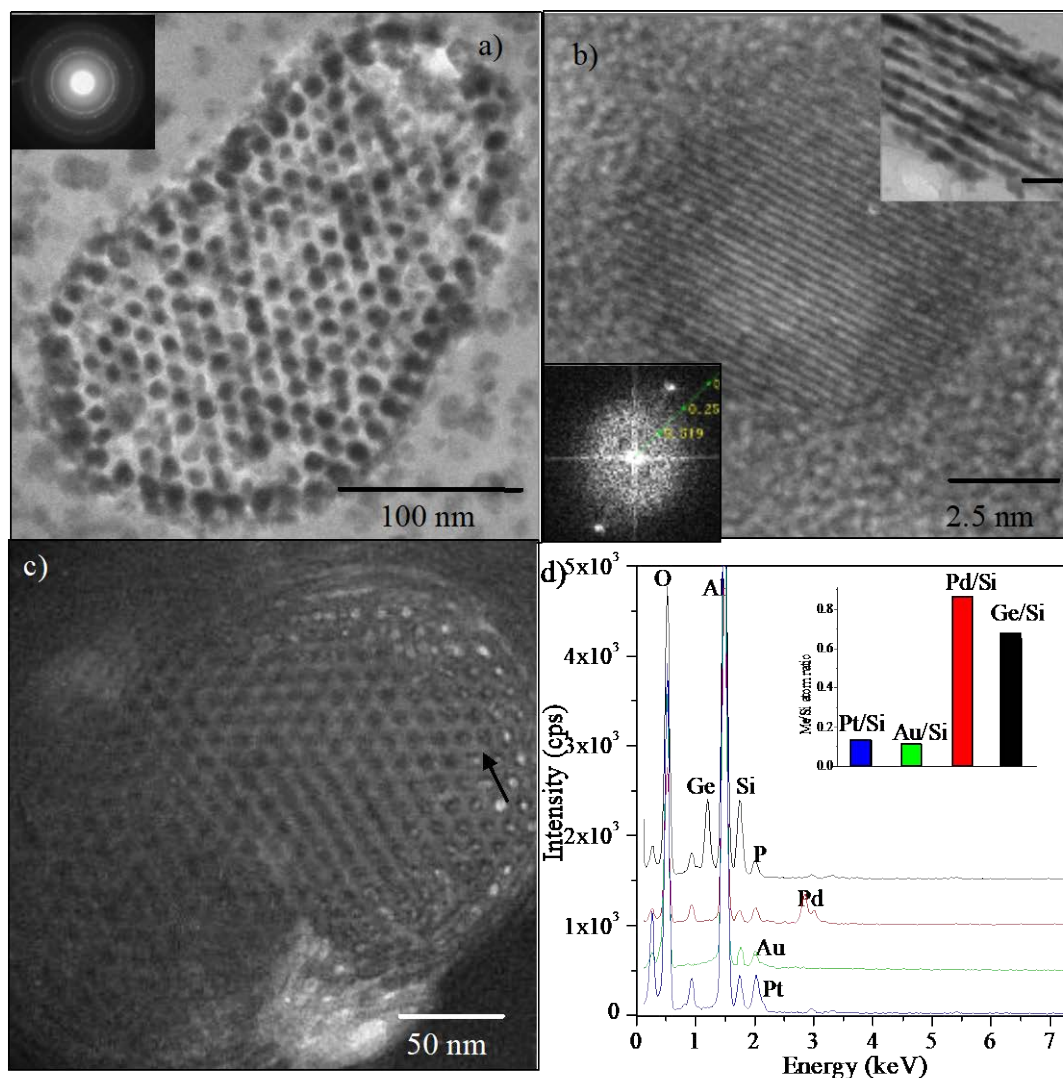
Figure 3. Pd-nanostructures prepared in non-calcined "columnar" mesostructured filaments. a) Plan-view TEM image (inset: corresponding SAED) and b) HRTEM image of one of the nanostructures shown in Figure 3a (inset: corresponding FFT and plan-view TEM image, scale bar 10 nm), and c) Ge-nanostructures in non-calcined columnar mesostructured filaments. d) Elemental analysis of the four different metal nanostructures discussed in this article.

REFERENCES

(1) Timp, G. *Nanotechnology*; 1st ed; Springer-Verlag: New York, **1999**.

(2) Heath, J. R.; Kuekes, P. J.; Snider, G. S.; Williams, R. S. *Science* **1998**, *280*, 1716.

(3) Petkov, N.; Bein, T. "Host-Guest-Systems based on Nanoporous Crystals" (Eds. F. Laeri, F. Schueth, U. Simon, M. Wark) Wiley-VCH, Weinheim, Germany, **2003,** 393-409.

(4) Klotz, M.; Albouy, P-A.; Ayral, A.; Menager, C.; Grosso, D.; Van der Lee, A.; Cabull, V.; Babonneau, F.; C. Guizard, *Chem. Mater.* **2000,** *120*, 1721.

(5) Besson, S.; Gacoin, T.; Ricolleau, C.; Jacquiod, C.; Boilot, J.-P. *NanoLetters* **2002**, *2*, 409

(6) Fan, H.; Yang, K.; Boye, D. M.; Sigmon, T.; Malloy, K. J.; Xu, H.; Lopez G. P.; Brinker, C. J. *Science* **2004**, *304*, 567.

(7) Li, G.C. Papadopolous, J. M. Xu and M. Moskovits, *Appl. Phys. Lett.* **1999**, *75*, 367.

(8) Y-G. Guo, C-J. Li, L-J. Wan, D-M. Chen, C-R. Wang, C-L. Bai, Y-G. Wang, *Adv. Funct. Mater.* **2003**, *13*, 626.

(9) Routkevitch, D.; Bigioni, T.; Moskovits, M.; Xu, J. M. *J. Phys. Chem. B* **1996**, *100*, 14037.

(10) Kulkarni, J. S.; Kazakova, O.; Erts, D.; Morris, M. A.; Shaw, M. T.; . Holmes, J. D. *Chem. Mater.* **2005**, *17*, 3615-3619.

(11) Kovtyukhova, N. I.; Kelley, B. K.; Mallouk, T. E.; *J. Am. Chem. Soc.* **2004**, *126,* 12738.

(12) Yamaguchi, A.; Uejo, F.; Yoda, T.; Uchida, T.; Tanamura, Y.; Yamashita T.; Teramae, N. *Nature Mater.* **2004**, *3*, 337.

(13) Wu, Y.; Cheng, G.; Katsov, K.; Sides, S. W.; Wang, J.; Tang, J.; Fredrickson, G. H.; Moskovits M.; Stucky, G. D. *Nature Mater.* **2004**, *3*, 816.

(14) Platschek, B.; Petkov, N.; Bein, T. *Angew. Chem. Int. Ed.* **2006**, *45*, 1134.

(15) Ryan, K. M.; Erts, D.; Olin, H.; Morris, M. A.; Holmes, J. D. *J. Am. Chem. Soc.* **2003**, *125*, 6284.

(16) Cott, D.; Petkov, N.; Morris, M. A.; Platschek, B.; Bein T.; Holmes, J. D. *J. Am. Chem. Soc.* **2006**, *128,*3920.

(17) Marlow, F.; Leike, I.; Weidenthaler, C.; Lehmann C. W.; Wilczok, U. *Adv. Mater.* **2001**, *13*, 3.

(18) Platschek, B.; Petkov, N.; Bein, T. in press.

(19) Cheng, J. Y.; Mayes A. M.; Ross*,* C. A. *Nature Mater.* **2004**, *3*, 823.

(20) Cohen, M. L. *Mater. Sci. Eng. C* **2001**, *15*, 1.

(21) Xia, Y.; Yang, P.; Sun, Y.; Wu, Y.; Mayers, B.; Gates, B.; Yin, Y.; Kim F.; Yan, H. *Adv. Mater.* **2003**, *15*, 353.

(22) Sakamoto, Y.; Fukuoka, A.; Higuchi, T.; Shimomura, N.; Inagaki, S.; Ichikawa, M. *J. Phys. Chem. B* **2004**, *108*, 853.

(23) Hanaoka, T.; Kormann, H-P.; Kroell, M.; Sawitowski, T.; Schmid, G. *Eur. J. Inorg. Chem.* **1998**, 807.

(24) Lahav, M.; Sehayek T.; Vaskevich, A.; Rubinstein, I. *Angew. Chem. Int. Ed.* **2003**, *42*, 5572.

(25) Petkov, N.; Stock, N.; Bein, T. *J. Phys. Chem. B* **2005**, *109*, 10737.

(26) Ziegler, K.; Ryan, K. M.; Rice, R.; Crowley, T.; Erts, D.; Olin, H.; Patterson, J.; Spalding, T. R.; Holmes, J. D.; Morris, M. A. *Faraday Discuss.* **2004**, *125*, 311.

(27) Ziegler, K. J.; Ryan, K. M.; Crowley, T. A.; Kulkarni, J.; Polyakov, B.; Erts, D.; Morris, M. A.; Holmes, J. D. *J. Mater. Chem.* **2004**, *14*, 585.

Table of Contents Figure

Nikolay Petkov, Barbara Platschek, Michael A. Morris, Justin D. Holmes* and Thomas Bein*

Chem. Mater. **2007**, *00*, 0000

Oriented Growth of Metal and Semiconductor Nanostructures within Aligned Mesoporous Channels

Different inclusion chemistries have been used to generate highly oriented metal and semiconductor nanostructues within the mesopores of aligned silica filaments. The crystallinity and continuity of the encapsulated nanostructures as a function of material and deposition technique are discussed.